



# **SEMICONDUCTOR EQUIPMENT**

## **THE EXTRION 220 PARALLEL SCAN MAGNET**

**R. Kaim and P. F. H. M. van der Meulen**

**Varian Ion Implant Systems  
Gloucester, MA 01930**

**Presented at the 8th International Conference on Ion Implant Technology  
July 30 – August 3, 1990  
Surrey, U.K.**

# THE EXTRION 220 PARALLEL SCAN MAGNET

R. E. Kaim, and P. F. H. M. van der Meulen

Varian Ion Implant Systems  
Gloucester, MA 01930

## Abstract

The design of the EXTRION 220 non-uniform field angle correction magnet is described. Implementation of the design is checked by making field maps of each magnet. The accuracy of beam parallelism has been verified by measuring the angular deviation of ion beam trajectories over the scanning width. It is shown that even small parallelism errors can have an effect on sheet resistance uniformity of high tilt angle implants.

## INTRODUCTION

Beam scanning in the EXTRION 220 is achieved by the combined action of an electrostatic deflector and a rectangular dipole magnet [1]. The field of the magnet varies in such a way as to convert the electrostatic angular scan into a one dimensional parallel scan. In this paper the design, construction and test of the non-uniform field magnet are discussed.

## MAGNET DESIGN

Figure 1 shows the geometrical layout of the magnet and electrostatic deflector. In designing the magnet, the following assumptions were made:

(i) The magnetic field in the x direction must vary as

$$B(x) = B_0 (1 + ax + bx^2) \quad [1]$$

where a and b are constants to be determined.

(ii) The effective width of the magnetic field in the z direction is constant for all values of x.

The values of the constants a and b in equation [1] were determined using the computer program RAYTRACE [2] which calculates the trajectories of charged particles in the presence of magnetic or electrostatic fields. The calculation was performed for the three trajectories shown in Fig. 1, corresponding to the center and sides of the scan for a 200mm wafer. Values of a and b were varied

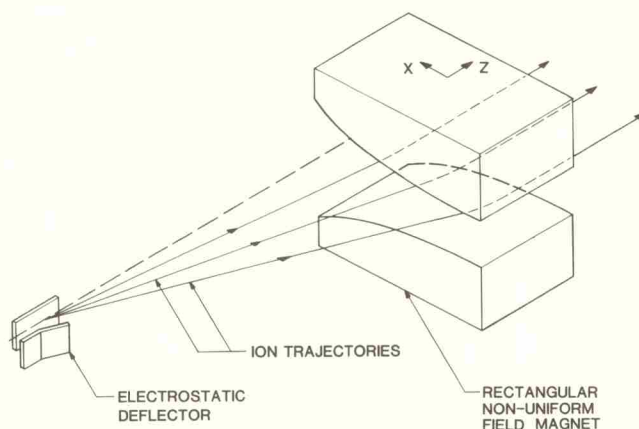


Figure 1 Schematic of E-220 parallel beam scanning.

iteratively in order to minimize the deviation from the z direction of all three trajectories emerging from the magnet.

Since the field inside a magnet is inversely proportional to the pole gap, the required pole curvature is governed by the equation:

$$D(x) = D_0 + (1 + ax + bx^2) \quad [2]$$

where  $D(x)$  is the pole gap.

## EFFECTIVE FIELD BOUNDARY

The difficulty with the design procedure outlined above is its assumption that the "magnetic width," or distance between effective field boundaries on each side of the poles, does not vary with  $x$ . The effective field boundary (EFB) is a measure of how much the magnetic field extends beyond the edge of the poles (see Fig. 2). The distance to the EFB is given by

$$L(x) = B(x,z) dx + B(\xi,0) \quad [3]$$

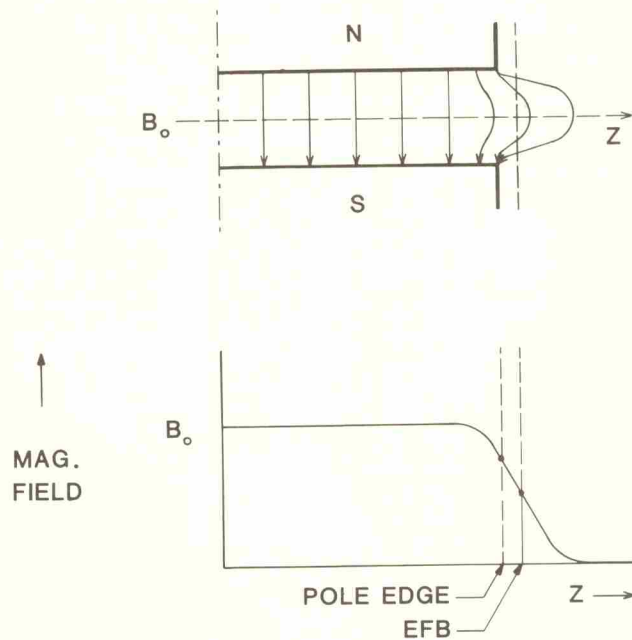


Figure 2 Concept of effective field boundary.

Figure 3a shows the expected effective field boundaries for the magnet depicted in Fig. 1. The distance from the pole edge to the EFB is roughly proportional to the pole gap [3], which means that the magnetic width is largest where the least deflection is required. Under these conditions the pole shape of equation [2] cannot produce the required parallel beam.

To correct for the "bulging" of the effective field boundaries, the magnet design incorporates field clamps whose purpose is to constrain the fringing fields. The field clamps consist of four flat plates fixed to the top and bottom return yokes on either side of the magnet. The effect of the clamps is to create a reversed magnetomotive force which constrains the magnetic field to very low values between each clamp pair, and thereby pushes the effective field boundaries closer to the poles. The goal is to achieve perfectly straight and parallel

EFBs as shown in Fig. 3b, so that the RAYTRACE calculation becomes valid and a parallel beam is produced. The extent to which the EFBs deviate from their desired location determines the accuracy of the beam parallelism achieved with the magnet.

## MAGNETIC FIELD MEASUREMENTS

In order to minimize the deviation of the EFB from its desired location, the gap between the field clamp plates has to be varied along the  $x$  direction - the smaller the gap the more the EFB is pushed in towards the pole edge. The optimum shape of the clamp plates was determined empirically for the first magnet by machining the clamps, measuring the resultant change in the EFB profile, and repeating the process until the deviation was sufficiently small.

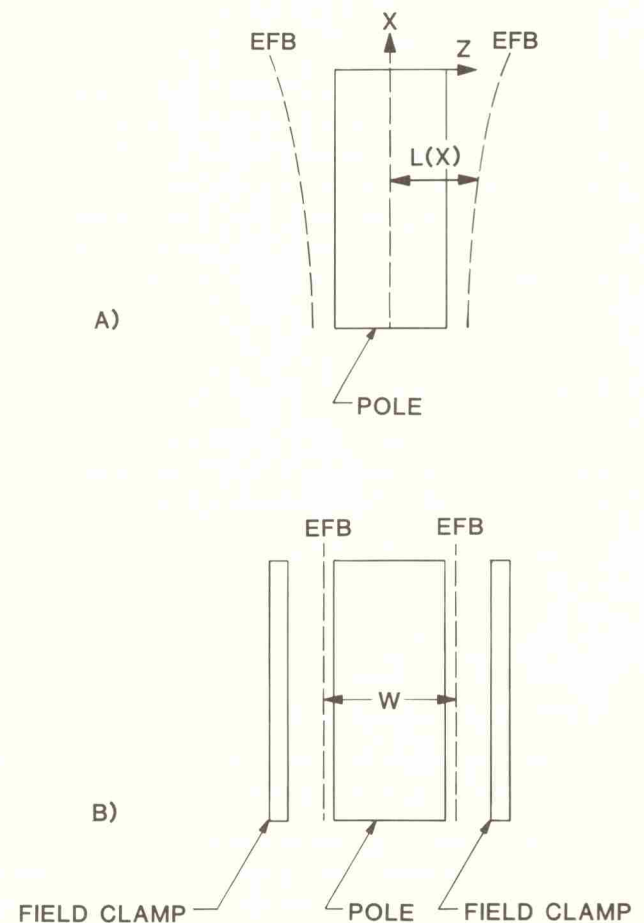


Figure 3 Effective field boundaries (a) with magnet as shown in Fig. 1, (b) with addition of field clamps.



For all subsequent magnets, the most critical measure of reproducibility and accuracy is the location of the EFBs. For each magnet the EFBs are measured, and the deviations from the design are required to be within limits which ensure that the specified beam parallelism will be achieved. The longitudinal deviation of the magnetic width  $W$ , for a sample of five magnets is shown in Fig. 4. The measurements were made at 25% and 100% of the maximum field, and it can be seen that the width depends on the field strength, illustrating the nonlinear nature of the magnetic effects causing deviation of the EFB. Nevertheless, these effects are reproducible from magnet to magnet, and amount to a few percent at most. Also shown at 25% field is the result for a prototype magnet which has different yoke and clamp dimensions from the later magnets.

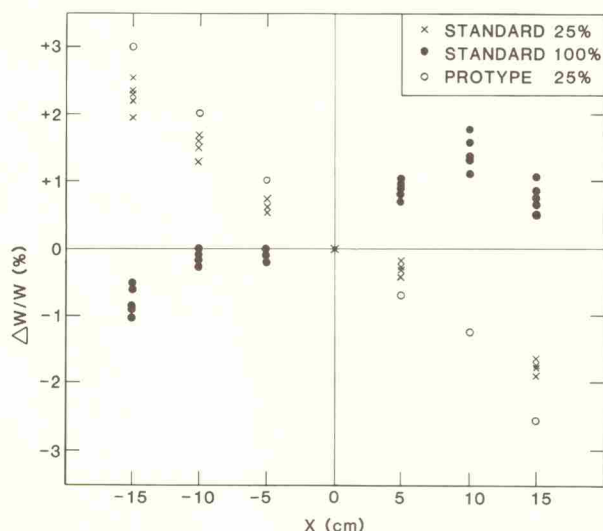


Figure 4 Deviation of magnetic width as a function of  $x$ . Measurements were made for 5 standard magnets and 1 prototype magnet at 25% and 100% of maximum field.

Another magnetic field measurement which is performed on each magnet is a check of the conformance to Equation [1] by measuring the field as a function of  $x$  at the line  $z=0$ . The deviation from equation [1] is required to be less than 0.5% over the working length of the magnet.

## BEAM PARALLELISM MEASUREMENTS

Once a magnet has been installed on the implanter, the accuracy of the beam parallelism can be measured in a number of ways. The most accurate method is illustrated in Fig. 5: two plates containing identical patterns of vertical slits are installed a fixed distance apart in the E-220 end station. The second plate is movable with a micrometer screw, and beam current transmitted through any pair of slits can be measured with a faraday plate. Using DC voltage on the electrostatic deflectors, the beam is steered sequentially through each slit in the first plate. The second plate is then moved to a position which maximizes beam transmission to the faraday plate, and the relative movement required provides a measure of the deviation from parallelism as a function of the position  $x$  of the first slit. Figure 6 shows measurements made for 40keV  $B^+$  and  $As^+$ , corresponding to low and high values of magnetic field. The deviations from parallelism are larger for  $B^+$  than for  $As^+$ , which is in agreement with the deviations of the magnetic width measurements shown in Fig. 4.

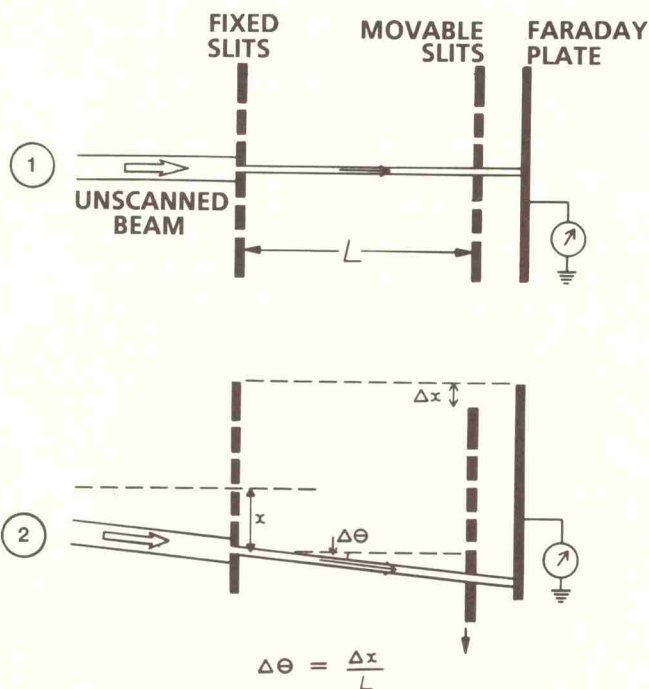


Figure 5 Method used to measure deviation of beam scan from parallelism.

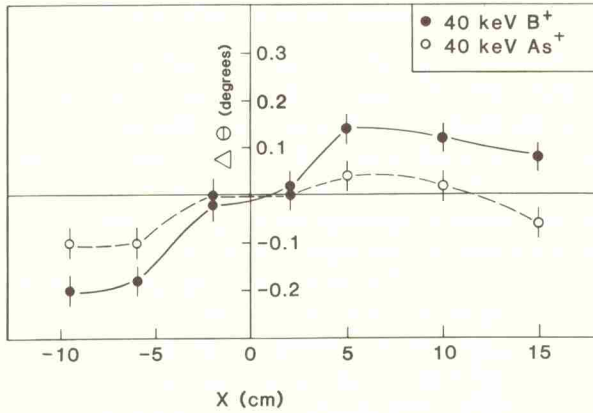


Figure 6 Deviations from parallelism of 40keV B and As (standard magnet).

### HIGH TILT ANGLE UNIFORMITY

There is a recent trend in ion implantation towards use of large tilt angles ( $60^\circ$  or more). For such large angles, errors in beam parallelism can cause degradation of the implant uniformity: for a tilt angle  $\theta$  and beam parallelism error  $\delta\Phi$  over the wafer diameter, the fractional change in dose from the center to the edge of the wafer is given by [4]:

$$X = 2 \tan \theta \tan \delta\Phi \quad [4]$$

It has been found that the inferior low-field performance of the prototype magnet (see Fig. 4) causes a noticeable degradation of the uniformity of high tilt angle boron implants. Figure 7 illustrates the result of an experiment in which wafers were implanted with boron at different tilt angles, but with the same effective dose and beam energy (i.e.

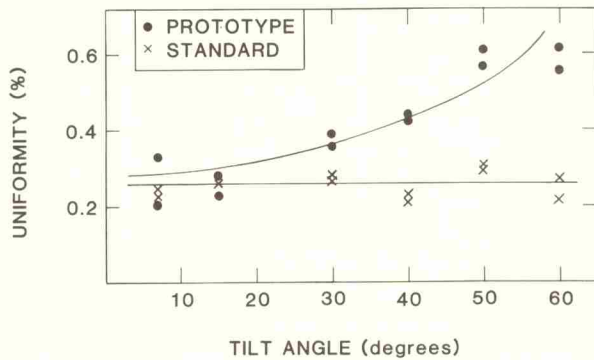
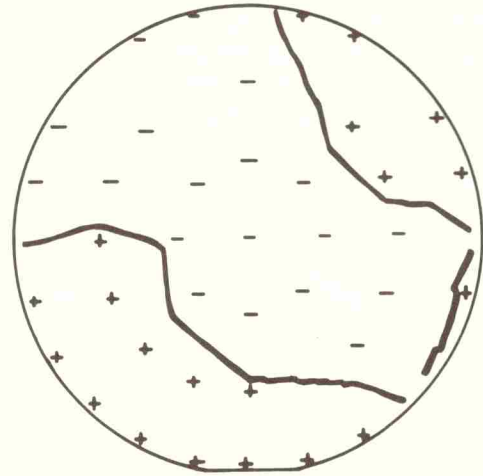
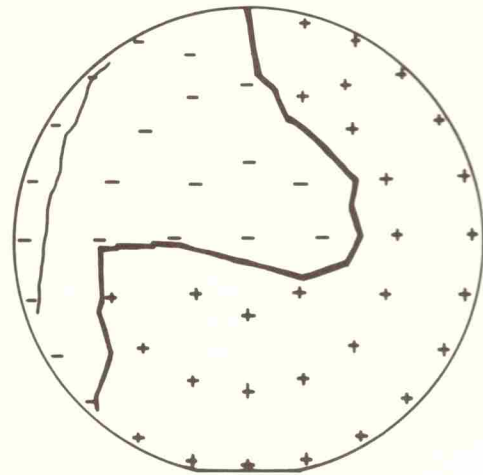


Figure 7 Implant uniformity as a function of tilt angle.

corrected by a factor  $1/\cos \theta$ ). The uniformity worsens with increasing tilt angle for the prototype magnet, but the effect is not apparent for an implanter using a magnet of the final design type. In Fig. 8 sheet resistance maps at  $50^\circ$  tilt are compared for the two magnets. Here it is seen that the degradation of uniformity for the prototype occurs in the direction of the horizontal beam scan, which is consistent with the effect of beam parallelism error.



a) STD DEV: 0.315



b) STD DEV: 0.58%

Figure 8 Sheet resistance maps for implants at  $50^\circ$  tilt. (Boron, 124.5keV,  $1.56 \times 10^{14}$  ions/cm<sup>2</sup>.) (a) Prototype magnet, (b) standard magnet.

## CONCLUSION

Measurements of the magnetic width provide an effective way to assure the accuracy and reproducibility of parallel scan magnets for the E-220. The parallelism may also be directly checked with an ion beam. Uniformity of high tilt implants can be a sensitive indicator of parallelism.

## REFERENCES

- [1.] D. W. Berrian, R. E. Kaim, J. W. Vanderpot and J. F. M. Westendorp, Nucl. Instr. and Meth. B37/38(1989)500.
- [2.] "RAYTRACE", S. Kowalski and H. A. Enge, 1985.
- [3.] H. A. Enge, Review of Scientific Instruments 35(1964)278.
- [4.] J. H. Keller, Radiation Effects 44(1979)71.